Putative metabolism of Ca. Accumulibacter via the utilization of glucose

Ziliani, Agustina; Bovio-Winkler, Patricia; Cabezas, Angela; Etchebehere, Claudia; Garcia, Hector A.; López-Vázquez, Carlos M.; Brdjanovic, Damir; van Loosdrecht, Mark C.M.; Rubio-Rincón, Francisco J.

DOI
10.1016/j.watres.2022.119446

Publication date
2023

Document Version
Final published version

Published in
Water Research

Water Research 229 (2023) 119446

Contents lists available at ScienceDirect

Water Research

journal homepage: www.elsevier.com/locate/watres

Putative metabolism of *Ca.* Accumulibacter via the utilization of glucose

Agustina Ziliani [a,b,*], Patricia Bovio-Winkler [c], Angela Cabezas [d], Claudia Etchebehere [c], Hector A. Garcia [a], Carlos M. López-Vázquez [a], Damir Brdjanovic [a,e], Mark C.M. van Loosdrecht [e], Francisco J. Rubio-Rincón [a]

[a] Department of Water Supply, Sanitation and Environmental Engineering, IHE Institute for Water Education, Westvest 7, 2611 AX Delft, The Netherlands
[b] Department of Environmental Microbiology, Swiss Federal Institute of Aquatic Science and Technology (Eawag), 8600 Dübendorf, Switzerland
[c] Laboratorio de Ecología Microbiana, Departamento de Bioquímica y Genómica Microbiana, Instituto de Investigaciones Biológicas Clemente Estable, Montevideo, Uruguay
[d] Instituto Tecnológico Regional Centro Sur, Universidad Tecnológica, Durazno, Uruguay
[e] Department of Biotechnology, Delft University of Technology, Julianalaan 67, 2628BC Delft, The Netherlands

ARTICLE INFO

Keywords:
Enhanced biological phosphorus removal
Wastewater with fermentable compounds
Glucose metabolism
Ca. Accumulibacter

ABSTRACT

Ca. Accumulibacter was the predominant microorganism (relative FISH bio-abundance of 67 ± 5%) in a lab-scale sequential batch reactor that accomplished enhanced biological phosphorus removal (EBPR) while using glucose and acetate as the carbon sources (1:1 COD-based ratio). Both organic compounds were completely anaerobically consumed. The reactor's performance in terms of P/C ratio, phosphorous release and uptake, and overall kinetic and stoichiometric parameters were on the high end of the reported spectrum for EBPR systems (100:9.3 net mg phosphate removal per mg COD consumed when using glucose and acetate in a 1:1 ratio). The batch tests showed that, to the best of our knowledge, this is the first time a reactor enriched with *Ca.* Accumulibacter can putatively utilize glucose as the sole carbon source to biologically remove phosphate (COD:P (mg/mg) removal ratio of 100:6.3 when using only glucose). Thus, this research proposes that *Ca.* Accumulibacter directly anaerobically stored the fed glucose primarily as glycogen by utilizing the ATP provided via the hydrolysis of poly-P and secondarily as PHA by balancing its ATP utilization (glycogen generation) and formation (PHA storage). Alternative hypotheses are also discussed. The reported findings could challenge the conventional theories of glucose assimilation by *Ca.* Accumulibacter, and can be of significance for the biological removal of phosphorus from wastewaters with high contents of fermentable compounds or low VFAs.

1. Introduction

The enhanced biological phosphorus removal (EBPR) process is widely used worldwide in municipal wastewater treatment plants. It is considered an efficient and more environmentally sustainable alternative to chemical methods (Coats et al., 2018; Oehmen et al., 2007). Theoretically, in an EBPR-activated sludge system, phosphorus is removed by polyphosphate-accumulating organisms (PAOs). PAOs utilize phosphorus beyond their growth requirements via the storing and hydrolysis of their polyphosphate pool, thus achieving greater phosphorus incorporation into the sludge mass (Barnard, 1975; Comeau et al., 1986).

To promote the growth of PAOs, the activated sludge system needs to be designed and operated so that these organisms' growth is stimulated and the consequent increase in phosphorus removal is achieved (Barnard et al., 2017). However, like with any microbiological process, the EBPR performance is prone to be affected by environmental and operational factors, such as a significant presence of detrimental microorganisms and physicochemical properties of the wastewater (Gebremariam et al., 2012; López-Vázquez et al., 2008).

Regarding the latter, glucose utilization has been a recurrent topic in the literature on the EBPR process (Cech and Hartman, 1993, 1990; Jeon and Park, 2000; Santos et al., 1999; Wang et al., 2002;). However, the attested consensus seemed that PAOs could not anaerobically uptake fermentable compounds such as glucose while promoting the subsequent phosphate uptake. On the contrary, the presence of glucose in EBPR systems was associated with an instability of the performance, as in the studies of Cech and Hartman (1990; 1993) and Begum and Batista (2012).

Different explanations were hypothesized for the deterioration of the

* Corresponding author.
E-mail address: agustina.ziliani@eawag.ch (A. Ziliani).

https://doi.org/10.1016/j.watres.2022.119446
Received 19 August 2022; Received in revised form 28 November 2022; Accepted 29 November 2022
Available online 30 November 2022

EBPR performance when glucose is used. In the first place, glucose was believed to select for an undesirable group of microorganisms, initially called G-bacteria, and later renamed glycogen accumulating organisms (GAOs), capable of accumulating glycogen without the release of phosphate (Mino et al., 1998). These organisms were believed to excessively proliferate under these circumstances, thus outcompeting the PAOs considering the fact that according to the metabolic model of Mino et al. (1994), they are able to produce PHAs with a positive net balance of one mole of ATP (Wang et al., 2010). On the other hand, the deterioration of the EBPR performance due to the absence of fermentative flanking species was first suggested by Randall et al. (1997). This study reported that PAOs could not ferment glucose during the anaerobic stage; hence, if the sugar was not pre-fermented by non-poly-P microorganisms, an EBPR failure could be expected. These two explanations correlate to the reports of Kong et al. (2004) and Nguyen et al. (2011), which inferred the canonical PAO *Ca.* Accumulibacter, usually considered vital in the EBPR process, cannot uptake glucose given the absence of encoding genes for its assimilation, a circumstance already hypothesized a priori by Wentzel et al. (1986). Nonetheless, a later metatranscriptomic study of *Ca.* Accumulibacter has stated differently (Oyserman et al., 2016).

Similarly, GAOs present the necessary genes for glucose assimilation. The same can be said about the fermentative putative PAO *Tetrasphaera*, as was first verified by Kong et al. (2005) and then further confirmed by Nguyen et al. (2011) and Kristiansen et al. (2013). However, the presence of fermentative PAOs such as *Tetrasphaera* could also prove to be detrimental to the EBPR process since an additional source of energy (as ATP) such as the one provided via fermentation could cease the poly-P hydrolysis. This theory is supported by Marques et al. (2017) and Rubio-Rincón et al. (2019). The latter suggested that neither *Tetrasphaera* nor *Ca.* Accumulibacter could significantly store phosphate while utilizing lactate as the primary carbon source. The reason behind this seems to be that no extra ATP is needed for storing lactate as PHA (hence no poly-P hydrolysis is required).

Despite this, several studies have reported a good EBPR performance while using glucose as the carbon source (Jeon and Park, 2000; Santos et al., 1999; Wang et al., 2002). In these reports, withal, different contradicting hypotheses were presented to explain the metabolism behind the recounted removal. Furthermore, due to the lack of microbial characterization in the previous studies, the role of *Ca.* Accumulibacter was not thoroughly elucidated or discussed. For this purpose, we conducted a long-term study by operating an anaerobic-aerobic sequential batch reactor (SBR) using glucose and acetate as carbon sources. We evaluated the results in terms of EBPR performance and the role of *Ca.* Accumulibacter in glucose-fed systems is analyzed and discussed.

2. Materials and methods

2.1. SBR operation

The biomass enrichment was carried out in a 3.0 L Applikon double-jacketed vessel operated as a sequencing batch reactor (SBR) employing the BioXpert software and an Applikon ADI 1030 bio-controller (Applikon, Delft, The Netherlands). The reactor's working capacity was 2.5 L, with an internal diameter of 12.5 cm and a water depth of 20.5 cm. The overall experimental setup is comparable to the one used by Rubio-Rincón et al. (2019).

Two different sludge sources were used as inoculum to have a varied initial microbial community: activated sludge from the biological nutrient removal plant of Harnaschpolder (Peuldreef 4, Den Horn, The Netherlands) and sludge provided by the Center for Microbial Communities (Department of Chemistry and Bioscience, Aalborg University, Aalborg, Denmark). The latter had a high abundance of the genus *Tetrasphaera*, whose presence was desired for their glucose utilization capability. A mixture of 400 mL of these two sources was used as inoculum.

The reactor was operated following cycles of 8 h. The cycles consisted of 3.5 h anaerobic, 3 h aerobic, and 1.5 h for settling and effluent withdrawal. The anaerobic conditions were induced by adding dinitrogen gas during the initial 25 min of the anaerobic phase and maintained by installing a water lock at the gas outlet. Before the addition of N_2 gas, the redox potential was – 200 mV/mA, which decreased to – 240 mV/mA after the supplement and reached – 380 mV/mA by the end of the anaerobic phase.

Each cycle commenced with adding 1.25 L of the synthetic medium, which maintained the HRT at 16 h. The SRT was set at 15 days, as reported by Rubio-Rincón et al. (2019), which in turn, with the mentioned cycles, resulted in an aerobic SRT of 6.25 d The temperature was set at 20 ± 1 °C and regulated by water recirculation through the reactor's double jacket using a Lauda-Brinkmann RE106 water bath chiller (Delran, United States). The pH was measured continuously by an AppliSens pH probe (Applikon, Delft, The Netherlands) and maintained at 7.0 ± 0.1 by the automatic supply of 0.4 M HCl or 0.4 M NaOH when needed. The dissolved oxygen concentration (DO) was set at 20% of the saturation level via an on/off function of the compressed air supply. The reactor was continuously stirred utilizing an overhead mixer set at 300 rpm through the anaerobic and aerobic phases.

Pseudo-steady-state conditions were considered to have been reached when the measurements of redox potential, VFA, and COD consumption and the MLVSS/MLSS ratio presented no significant changes (above 1%) in 3 SRTs (45 days). Phosphorus removal was also contemplated but within a 10% change rate.

2.2. Batch tests

Batch tests were carried out once the reactor reached pseudo-steady-state conditions using glucose or acetate individually as the carbon source. The tests were conducted by adding 200 mL of mixed liquor from the parent reactor (taken after the aerobic phase) into smaller double-jacketed reactors with a working capacity of 0.5 L and connected to an Applikon ADI 1030 bio-controller. The sludge was kept aerobically until the test started, and the same cycles mentioned before were repeated, that is, 3.5 h of anaerobic phase and 3 h of aerobic phase. The temperature was controlled at 20 °C, pH at 7.0, and agitation at 300 rpm. Samples for PO_4-P, $NH_4^+ - N$, DOC, and VFAs were taken every 10 min, while MLSS/MLVSS were measured at the beginning and end of each phase.

Oxygen uptake rate (OUR) profiles were also determined. The sludge was recirculated via a biological oxygen monitor, which included a DO probe. The recirculation was intermittently re-started once the dissolved oxygen concentration stabilized or reached 2 mg/L and taken up to about 8 mg/L to assess the DO profile decline again.

2.3. Synthetic media

The concentrations per liter were: 400 mg COD (acetate and glucose in a 1:1 ratio), 50 mg $PO_4^{3-} - P$, 28 mg $NH_4^+ - N$, 50 mg SO_4^{-2}, 19 mg K^+, 15 mg Mg^{2+}, 4 mg Ca^+, 1 mg yeast extract, 20 mg N-allylthiourea (ATU) (to prevent nitrification since phosphorus removal was the target of the study), and 300 μL of the trace elements solutions prepared following the research of Smolders et al. (1994a). The 1:1 acetate-glucose ratio was used to promote the enrichment of PAO-like organisms and to study the possible symbiosis among different genera (acetate-utilizing and glucose-utilizing bacteria). For the batch tests, a 200 mg/l COD concentration of either glucose or acetate was used (other concentrations remained unchanged).

2.4. Chemical analyses

MLSS, MLVSS, orthophosphate (PO_4-P), ammonia ($NH_4^+ - N$), and total organic carbon (TOC) were measured weekly at the start of each

differential phase for one cycle following the standard methods described by APHA et al. (2005). The volatile fatty acids (VFAs) were measured using a Varian 460 gas chromatograph (Nieuwegein, The Netherlands).

2.5. Stoichiometric and kinetic parameters

The net phosphate release (mg PO_4-P/L) and phosphate release per VFA consumption ratio (mol P/mol C) were calculated considering the concentration value when the carbon source ran out since carbon was depleted in every test. Thus, the P release due to maintenance purposes was excluded from the observed phosphate release.

The kinetic parameters of interest were calculated using the linear regression method reported in Smolders et al. (1995) research, where the maximum volumetric rates relate to the slope of the applicable data set. No less than 5 experimental points were used for these calculations. The phosphate biomass content (f_P) was calculated following the study of Smolders et al. (1996) by using the following equation:

$$f_P = \frac{\text{phosphate removed}}{\text{observed growth yield} \cdot \text{COD consumed}} \text{ (mg P/mg VSS)}$$

2.6. FISH analysis

Fluorescence in situ hybridization (FISH) analyses were carried out to characterize the enriched culture and determine the most relevant communities' relative abundances. The *Ca.* Accumulibacter genus was targeted by the probes PAO 462, PAO 651, and PAO 846, which combined an 89% coverage of the named genus (Crocetti et al., 2000). Since the genus *Propionivibrio* was among the most abundant in the 16S rRNA gene amplicon sequencing results, the probe PAO 651 was also used by itself to rule out the possible overestimation of *Ca.* Accumulibacter, as suggested by Albertsen et al. (2016), thus also decreasing the coverage to 71% of the species from the genus *Ca.* Accumulibacter. In addition, the genus *Ca.* Competibacter and the GAO community were targeted with the probes GAOQ 431 and GAOQ 989 (Crocetti et al., 2002). When it comes to the genus *Tetrasphaera*, only probes with confirmed coverage and specificity were selected for the current research. To span the three clades of the genus, Tet2–842, Tet2–174, and Elo1–1250 were chosen (Nguyen et al., 2011). *T. japonica*, which does not belong to any clade, was covered by the probe Actino_1011 (Liu et al., 2001).

Vectashield anti-fade medium with DAPI was used to preserve the sample's fluorescence and stain all organisms, as suggested by Nielsen (2009) (Vector Laboratories, CA, USA). An Olympus BX51 microscope and the Cell Dimensions 1.5 software were used. For the quantification of each probe, 20 random pictures were analyzed, and the standard error of the resulting mean was calculated considering the standard deviation and dividing it by the square root of the number of images analyzed.

2.7. 16S rRNA gene amplicon sequencing analyses

The genomic DNA (gDNA) was extracted using the QIAamp® PowerFecal® DNA Kit (QIAGEN Inc., CA, USA) following the manufacturer's protocol. The extracted gDNA was measured using a Qubit™ 3.0 Fluorometer and the Qubit™ dsDNA BR Assay Kit by Invitrogen (Thermo Fisher Scientific, The Netherlands).

The extracted gDNA from the reactor and the inoculum were sequenced using the primers 341F (5′-CCTACGGGNGGCWGCAG-3′) and 805R (5′-GACTACHVGGGTATCTAATCC-3′), designed for the regions V3-V4 of general bacteria (Herlemann et al., 2011) and performed on an Illumina MiSeq platform by Macrogen Inc. (Seoul, Korea) (Illumina Reagent Kit v2).

The resulting raw sequences (244,774 in total) were processed using the "Quantitative Insights Into Microbial Ecology" pipeline (QIIME2 2021.4 release). The sequencing reads were screened using the DADA2 "divisive amplicon denoising algorithm" plugin. This step filters out noise and corrects errors in marginal sequences, removes chimeric sequences and singletons, and finally dereplicates the resulting sequences, resulting in 2015 high-resolution amplicon sequence variants (ASVs) for downstream analysis. The consensus sequences for the ASVs were classified with a classify-sklearn classifier trained against the pre-trained classifier MiDAS 4.8.1 database (Dueholm et al., 2021).

The subsequent statistical analyses were performed in R, version 4.1.0 (R Core Team 2021). The biom file from QIIME2 was imported and analyzed through a phyloseq-modified workflow (McMurdie and Holmes, 2013). Sequences were rarefied to the lowest number of sequences per sample ($n = 57{,}981$ sequences). Heatmaps were generated using ampvis2 (v.2.6.5).

2.8. Proteome analysis

Sample preparation and database search for metaproteomic analysis was performed as described by (Kleikamp et al., 2020). Shotgun proteomic raw data were matched against a global bacterial database downloaded from UniprotKB using a 2-round search approach.

2.9. Metagenome sequencing

Metagenomes were shotgun sequenced on an Illumina Nova Seq 6000 Platform (2 × 150 bp) at Novogene Corporation Inc. (Sacramento, CA). The yield was approximately 12 Gb (~6Gb/sample) of raw short-read sequences per library. The raw amplicon and metagenome sequences were deposited under the NCBI BioProject PRJNA809015 (https://www.ncbi.nlm.nih.gov/sra/PRJNA809015).

2.10. Metagenomic assembly, binning of contigs, classification, and annotation

The global quality of metagenomic reads was checked using FastQC (v0.11.9). The reads were trimmed to remove adapters and bases below a quality score of 25 using Trimmomatic (v0.39) (Bolger et al., 2014). Then, clean reads from each sample were pooled and assembled into contigs using MEGAHIT v1.1.3 with the options: –k-min 43 –k-max 111 –k-step 4 (Li et al., 2016).

To obtain metagenome-assembled genomes (MAGs), binning and refinement were performed with metaWRAP v1.3.2 (Uritskiy et al., 2018). The completeness and contamination of MAGs were estimated using CheckM (v1.0.18). Taxonomy was assigned to each MAG based on the GTDB-Tk v1.7.0 and the Genome Taxonomy Database (GTDB) r202 (Parks et al., 2020). MAGs were annotated with the "annotate" function of EnrichM v0.5.0 (https://github.com/geronimp/enrichM) using the Kyoto Encyclopedia of Genes and Genomes (KEGG) Orthologies (KOs) to reconstruct metabolic pathways (Kanehisa and Goto, 2000). EnrichM's "classify" function was used to calculate the completeness of KEGG modules.

3. Results

3.1. Acclimatization of the biomass

The reactor was operated under the described conditions for over 100 days. Pseudo-steady-state conditions were reached around day 60 (Fig. 1), and putative fermentative conditions were reached (~ −380 mV/mA) on day 15. The adaptation/selection process, as checked through the biomass growth, took less than 10 days. During the pseudo-steady-state operation, a high net P removal efficiency of around 30 to 40 mg PO_4-P/L was consistently maintained, and the fed carbon sources were entirely anaerobically consumed. The observed biomass yield was 0.28 g VSS/g COD, giving a phosphate biomass fraction content of 0.30 mg P/mg VSS.

As mentioned, all carbon sources were utilized entirely during the anaerobic stage. The COD was consumed at a rate of 50.0 mg COD/g VSS

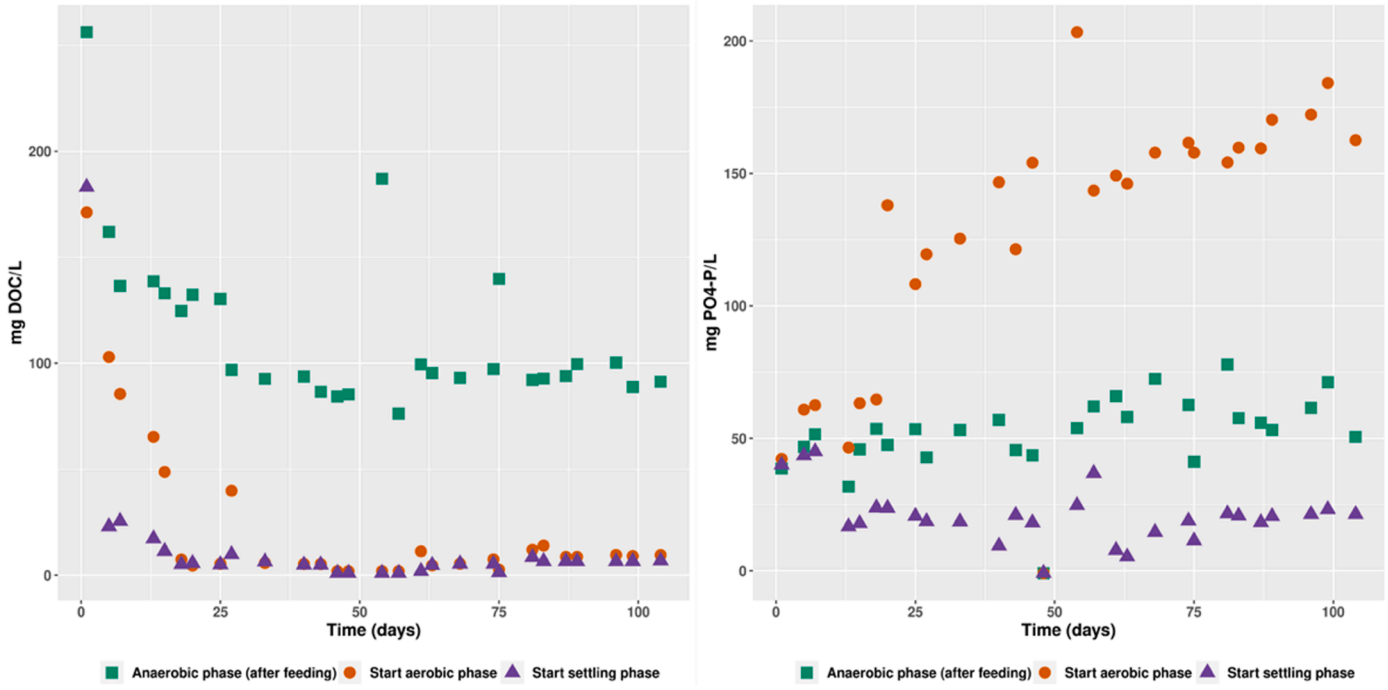

Fig. 1. DOC (left) and ortho-phosphate (right) profiles throughout the reactor's operation. On the same day, three samples were taken: one at the start of the anaerobic phase after the 5 min of feeding (squares), one at the beginning of the aerobic phase (circles), and the last one at the start of the settling phase (triangles).

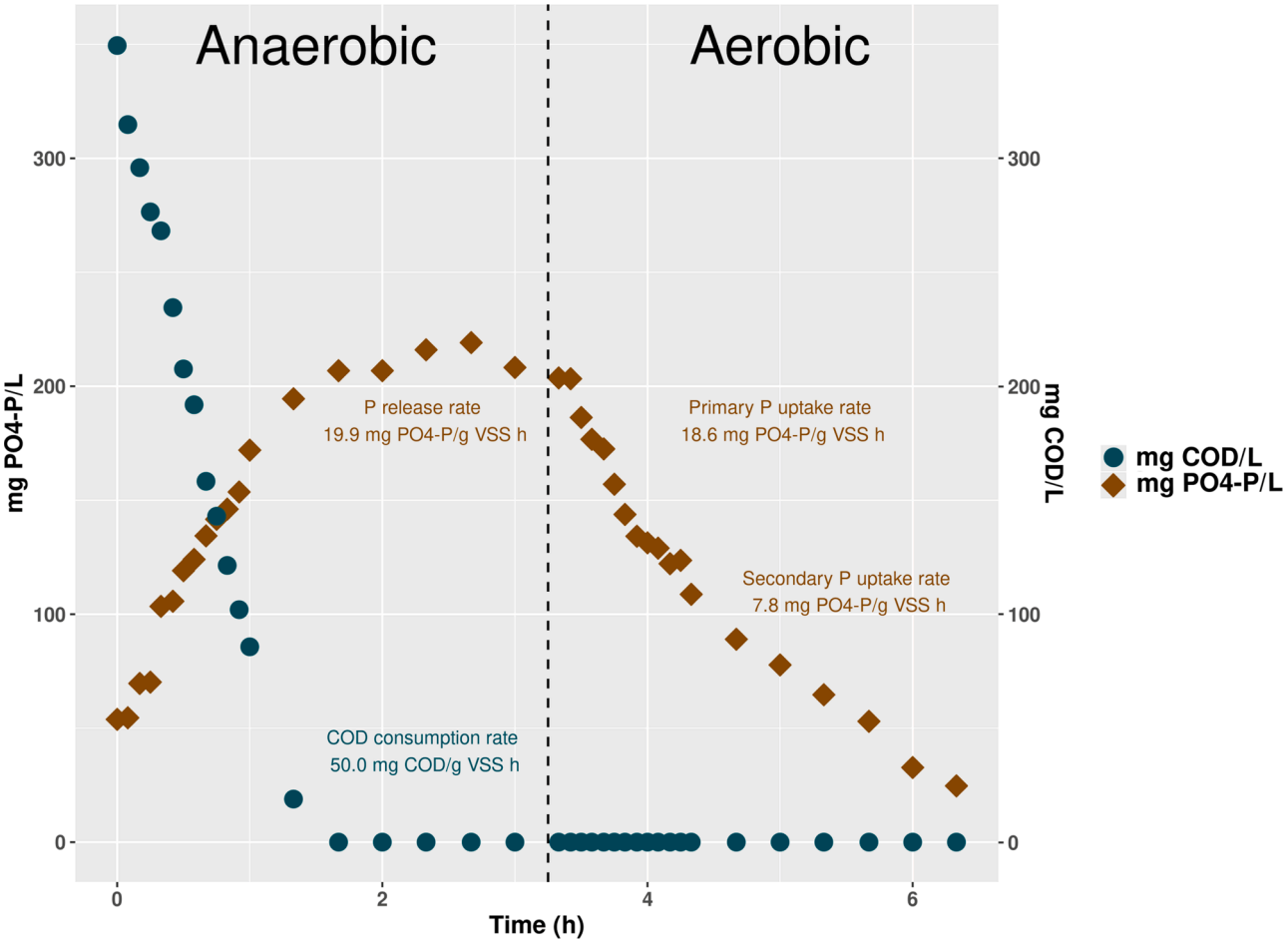

Fig. 2. COD (circles) and ortho-phosphate (diamonds) profiles for the cycle test of the reactor, along with the maximum specific rates (in mg COD/g VSS h or mg PO4-P/g VSS h). The anaerobic phase was 3.5 h, while the aerobic was 3 h.

h (Fig. 2). As expected, the anaerobic carbon consumption was correlated with an anaerobic phosphate release of 153.0 mg PO_4-P/L at 19.9 mg PO_4-P/g VSS h (Table 1). Once all carbon was consumed, the phosphate release diminished to 2.7 mg PO_4-P/g VSS h. Overall, the phosphate release per carbon consumed was 0.45 (mol P/mol C).

During aerobic conditions, the biomass was able to uptake 195 mg PO_4-P/L at a primary rate of 18.6 mg PO_4-P/g VSS h (for the first aerobic hour) and 7.8 mg PO_4-P/g VSS h the remaining time. Hence, with these results, the overall removal was 29 mg PO_4-P/L. In addition, the ratio of mg COD anaerobically consumed per mg phosphorus aerobically uptake of the cycle test was 100:9.3.

3.2. Individual assessment of acetate and glucose on the microbial metabolism

When only acetate was used as the carbon source, the fed 200 mg COD/L were fully consumed after 100 min of the anaerobic phase at a rate of 40.1 mg COD/g VSS h (Fig. 3, Table 1). As observed before, acetate's putative intracellular accumulation was correlated with a net phosphate release of 100 mg PO_4-P/L at a rate of 19.1 mg PO_4-P/g VSS h when acetate was still present in the liquid and a rate of 0.2 mg PO_4-P/g VSS h afterward. The overall P/VFA ratio was 0.52 (mol P/mol C). In line with the phosphate release and acetate accumulation, the VSS/TSS ratio changed from 0.81 to 0.87 at the start and end of the anaerobic phase, respectively.

During the aerobic phase, a net phosphorus uptake of 83.7 mg PO_4-P/L at a primary rate of 12.5 mg PO_4-P/g VSS h (first aerobic hour) and at a secondary rate of 6.4 mg PO_4-P/g VSS h in the remaining P up taking period were measured. Combining these two results, the batch test did not display overall phosphorus removal since the concentration after the aerobic phase (59 mg PO_4-P/L) was higher than at the beginning of the test (40 mg PO_4-P/L). The O_2:COD ratio was 0.6.

On the other hand, when only glucose was used as the carbon source, the fed 200 mg COD/L were completely consumed after 140 min of the anaerobic phase at a rate of 5.6 mg COD/g VSS h (Fig. 3, Table 1). The interrelated net phosphate release of 48.6 mg PO_4-P/L at a rate of 9.8 mg PO_4-P/g VSS h while the carbon source was still present in the liquid was followed by a release at the diminished rate of 2.4 mg PO_4-P/g VSS h. Hence, the P/VFA ratio was 0.26 (mol P/mol C). Once again, the phosphate release and glucose consumption were in accordance with the TSS/VSS ratio, which changed from 0.73 at the start of the anaerobic phase to 0.81 recorded by its end.

The net P uptake was 65 mg PO_4-P/L h, with a release rate of 7.7 mg PO_4-P/g VSS g for the first hour and 3.1 mg PO_4-P/g VSS for the remaining aerobic time. Coalescing both results, the net P removal for this experiment was 5 mg PO_4-P/L, corresponding to 15% of the phosphorus at the beginning. The O_2:COD ratio was 0.5.

3.3. Characterization of the microbial community

Fluorescence in situ hybridization (FISH) and 16S rRNA gene-based amplicon sequencing were performed to identify the predominant microorganisms of the obtained culture and assess their relative abundance. *Ca.* Accumulibacter was the most abundant of the targeted populations, with a relative abundance of 67 ± 5% compared to the whole microbial population (targeted by DAPI), followed by *Ca.* Competibacter (probes GAOQ431 and GAOQ989), which accounted for 32 ± 4% (Fig. 4, Table 2). To gage the possible overestimation of *Ca.* Accumulibacter by the closely related putative GAO *Propionivibrio*, the probe PAO651 was also used by itself (Albertsen et al., 2016). In this case, the result was 49 ± 4%.

When evaluating the Gram-positive bacteria, the relative abundance of Actinobacteria (probe Actino_1011) was 8 ± 1%, while the three probes targeting the genus *Tetrasphaera* accounted for, in total, 10% (probes Tet2–842, Tet2–174, and Elo1–1250).

The 16S rRNA gene amplicon sequencing results supported the examined trends. Regarding the phyla, the most abundant ones in the reactor sample were Proteobacteria, Patescibacteria, and Bacteroidota, respectively, representing 83% of the community (Fig. 5).

The most abundant family in the culture was *Rhodocyclaceae*, in which the genus *Ca.* Accumulibacter was the predominant member, with a relative abundance of 17.3, regarding the accounted ASVs (Fig. 5). The latter signified a sharp increase from the 2.2% present in the inoculum. Once again, members of the family *Competibacteraceae*, specifically the genus *Ca.* Competibacter were also among the most abundant, both in the inoculum and the obtained culture. In the latter, the relative abundance of the genus was 10.4%. Different members of the family *Saccharimonadaceae* also increased significantly, from an initial undetectable abundance to a considerable 10.4%. The genus *Propionivibrio* amounted to 4.7% from an initial 0.9%, while *Tetrasphaera* remained constant at 0.4% (data not included).

3.4. Possible metabolic pathways

The proteomic analysis exhibited the predominance of the genus *Ca.* Accumulibacter, supporting the results from the FISH analyses and the 16S rRNA gene amplicon sequencing, and in line with the good EBPR performance that hinted a high abundance of PAO-like organisms. Of the total expressed proteins, on average, 52% corresponded to this genus and, more specifically, to three species, *Accumulibacter phosphatis* strain UW-1, *Accumulibacter aalborgensis*, and *Accumulibacter* sp. The GAO bacteria *Competibacter denitrificans* was second (6.1%), followed by *Contendobacter odensis* and *Propionivibrio aalborgensis* (4.6%). Thus, these four genera amounted to almost 70% of the expressed proteins. Lastly, 0.18% of the proteins corresponded to the putative PAO genus *Tetrasphaera*, represented by *T. australiensis, T. japonica*, and *T. elongata*.

All the enzymes involved in the tricarboxylic acid cycle, as well as the glyoxylate shunt (malate synthase and isocitrate lyase) (data not shown) and in the glycolysis (EMP pathway), were present in the culture and among the most abundant of the expressed proteins (Table 3). The latter relates to the deep fermentation conditions reached during the reactor's operation. More specifically, except for the glucokinase required for the first step of glycolysis (converting glucose into glucose-6-phosphate), *Ca.* Accumulibacter was the only genus expressing all the

Table 1
Anaerobic, aerobic, and overall stoichiometric and kinetic parameters that were calculated for the different tests.

	Anaerobic			Aerobic			Overall process			
	Net P release (mg PO_4-P/L)	$q^{MAX}_{PO_4,AN}$ (mg PO_4-P/g VSS h)	$q^{MAX}_{COD,AN}$ (mg COD/ g VSS h)	Net P uptake (mg PO_4-P/L)	$q^{MAX}_{PO_4,Ox}$ (mg PO_4-P/g VSS h)	O_2/COD ratio (mg O_2/mg COD)	P/C ratio (mg PO_4-P /mg COD)	P/C ratio (mol P/ mol C)	Net P removal (mg PO_4-P/L)	Net P removal/COD consumed (mg PO_4-P/mg COD)
Cycle test	153.0	19.9	50.0	194.5	18.6 7.8	–	0.44	0.45	29.1	0.08
Batch test Glucose	48.6	9.8	5.6	64.6	10.4 4.2	0.5	0.24	0.26	4.8	0.02
Batch test Acetate	100.0	19.1	40.1	83.7	12.5 6.4	0.6	0.50	0.52	0	–

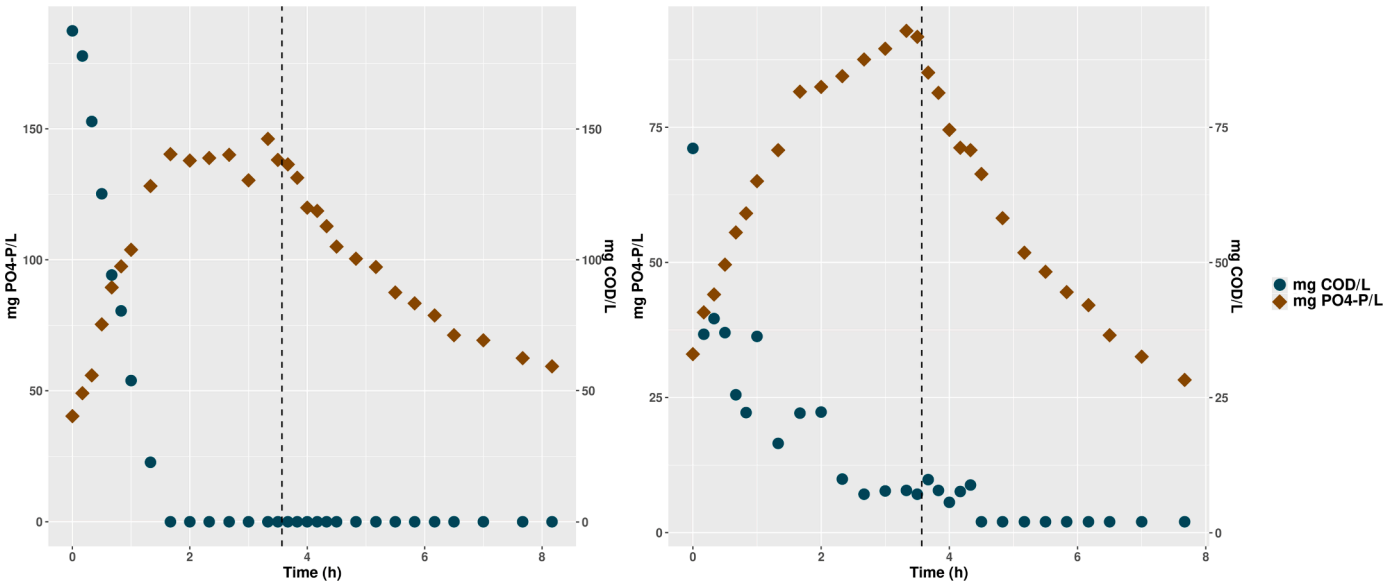

Fig. 3. COD and ortho-phosphate profiles for the batch tests with acetate (left) and glucose (right) as sole carbon sources.

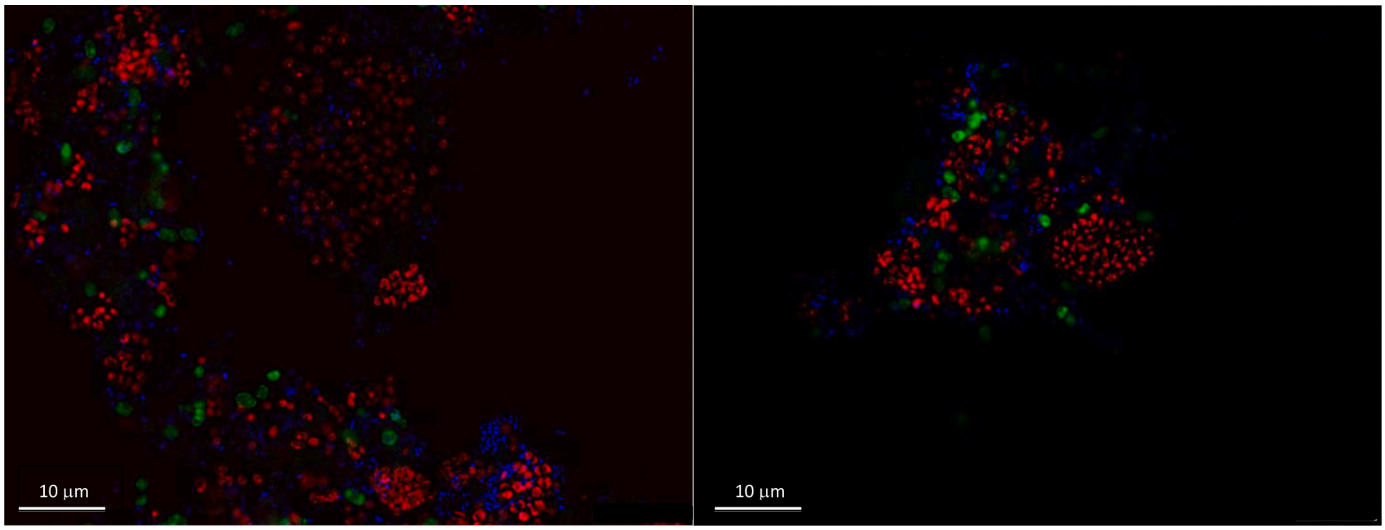

Fig. 4. Microbial characterization through FISH analysis. In blue, all organisms (DAPI), in red (CY3), PAO cluster (PAO 462, 651, and 846), and in green, (FAM) Ca. Competibacter (GAOQ 431 and 989). (For interpretation of the references to colour in this figure legend, the reader is referred to the web version of this article.)

enzymes necessary for the named pathways. The glucokinase was not characterized in any of the most abundant genera, and its abundance in other genera was significantly low (0.1%). Contrarily to the EMP pathway, none of the enzymes required for the Entner-Doudoroff (ED) glycolysis pathway were detected in the most abundant genera.

Regarding the storage polymers, all of the enzymes involved in the glycogen synthesis were present for *Ca.* Accumulibacter but not for the other abundant genera. The enzymes involved in the poly-hydroxybutyrate (PHB) synthesis acetyl-CoA C-acyltransferase (*phaA*), acetoacetyl-CoA reductase (*phaB*), and PHB synthase (*phaC*) were all detected in the genus *Ca.* Accumulibacter and the species *Competibacter denitrificans* and *Contendobacter odensis*, with the addition of the enoyl-CoA hydratase (*phaJ*) detected in the first two. In addition, the enzymes methyl malonyl-CoA mutase and propionyl-CoA carboxylase, involved in the synthesis of polyhydroxyvalerate (PHV) and polyhydroxy-2-methyl butyrate (PH2MB) from succinyl CoA, were also detected (Table 3).

3.5. Metagenomic assembled genomes

Using samples from different stages of the reactor's operation (once it had reached pseudo-steady-state conditions), it was possible to retrieve 61 metagenomic assembled genomes (MAGs) with completeness above 50% and less than 10% of contamination. The 11 MAGs of interest annotated with KEGG orthology considering the results of the 16S rRNA gene analysis and the metaproteomic analysis, along with its genome size, completeness, and taxonomic annotation, among other indicators, are summarized (Table 4). It was possible to annotate 2 MAGs belonging to the *Rhodocyclaceae* family, 3 of *Competibacteraceae*, and 6 from *Saccharimonadaceae*. No member of the *Tetrasphaera* genus (or the *Intrasporangiaceae* family) was annotated.

The annotated MAG of *Ca.* Accumulibacter encoded for the majority of the genes involved in the glycolysis (EMP pathway), except for the *TPI* (triosephosphate isomerase) and the *PGK* (phosphoglycerate kinase) (Table 5). The *glk* gene (glucokinase) was encoded in the MAG of *Ca.* Accumulibacter and *Ca.* Propionivibrio, but not in the remaining 9 MAGs of interest. Regarding acetate uptake and utilization, the MAGs of

Table 2
Relative abundances of the targeted microbial communities assessed through FISH analysis as compared to the whole microbial population (targeted by DAPI), along with the specificity of the utilized probes.

Probe	%	Standard error	Specificity of probe	Reference
PAO462 PAO651 PAO846	67	5	PAO cluster	Crocetti et al. (2000)
GAOQ431 GAOQ989	32	4	*Ca.* Competibacter phosphatis	Crocetti et al. (2002)
PAO651	49	4	*Accumulibacter* sp.	Crocetti et al. (2000)
Actino_1011	8	1	*Actinobacteria* (including *T. japonica* and related clones)	Liu et al. (2001)
Tet 2–174	1	0.4	*T. jenkinsii, T. australiensis, T. veronensis* and *Candidatus* N. limicola	Nguyen et al. (2011)
Elo 1–1250	4	0.3	*T. elongata* and related clones	Nguyen et al. (2011)
Tet 2–842	5	2	Clones related to *T. jenkinsii, T. australiensis*, and *T. veronensis*	Nguyen et al. (2011)

Ca. Accumulibacter and *Ca.* Competibacter were the only ones that encoded the complete pathway (*actP, acs, pta*, and *ackA*).

Most MAGs encoded the complete glycogen synthesis pathway, except for the *Saccharimonadaceae* family MAGs. On the other hand, the pyruvate oxidation pathway (from pyruvate to acetyl CoA) was encoded in *Ca.* Accumulibacter's MAG and none of the MAGs of interest encoded the glycolysis' ED pathway.

The annotated MAG of *Ca.* Accumulibacter encoded the most amount of PHA synthesis-related genes, with *phaA, phbB*, and *phbC* all present. These genes were also accounted for in the MAGs of *Ca.* Contendobacter odensis and the two *Ca.* Competibacter. However, they were not found in the MAG of *Ca.* Propionivibrio (MAG level of completeness of 97.5%). Furthermore, as for the phosphorus removal mentioned before, the MAG of *Ca.* Accumulibacter encoded all necessary genes (e.g., *ppx, pap, adk, ppk1*, and *Pit)*.

Regarding the 6 annotated MAGs belonging to the *Saccharimonadaceae* family, all of them lacked the first three glycolysis genes (EMP pathway) and encoded only one gene for the ED pathway and glycogen synthesis. No encoding genes were found concerning acetate uptake, glucose uptake, acetate utilization, pyruvate oxidation, PHA synthesis, or glucose fermentation (Table 5).

4. Discussion

4.1. Biological phosphorus removal using glucose-acetate fed

As aforementioned, the presence of glucose in the influent of an EBPR process was usually associated with a disruption of the process since *Ca.* Accumulibacter was considered unable to anaerobically uptake fermentable compounds. Nevertheless, in our study, the performance of the reactor fed with glucose and acetate (1:1 ratio) was comparable to a reactor with a noteworthy EBPR performance in terms of phosphorus release, uptake, and overall kinetic as well as stoichiometric parameters. When comparing these values with reported values, the specific P release of the parent reactor and the batch test with acetate fell on the high end of the reported spectrum for EBPR full-scale systems (Table 6). The COD uptake rate of the reactor was also higher than the reported for full-scale EBPR systems, with a difference ranging from 6 to 82%, considering, respectively, the lowest and highest reported values

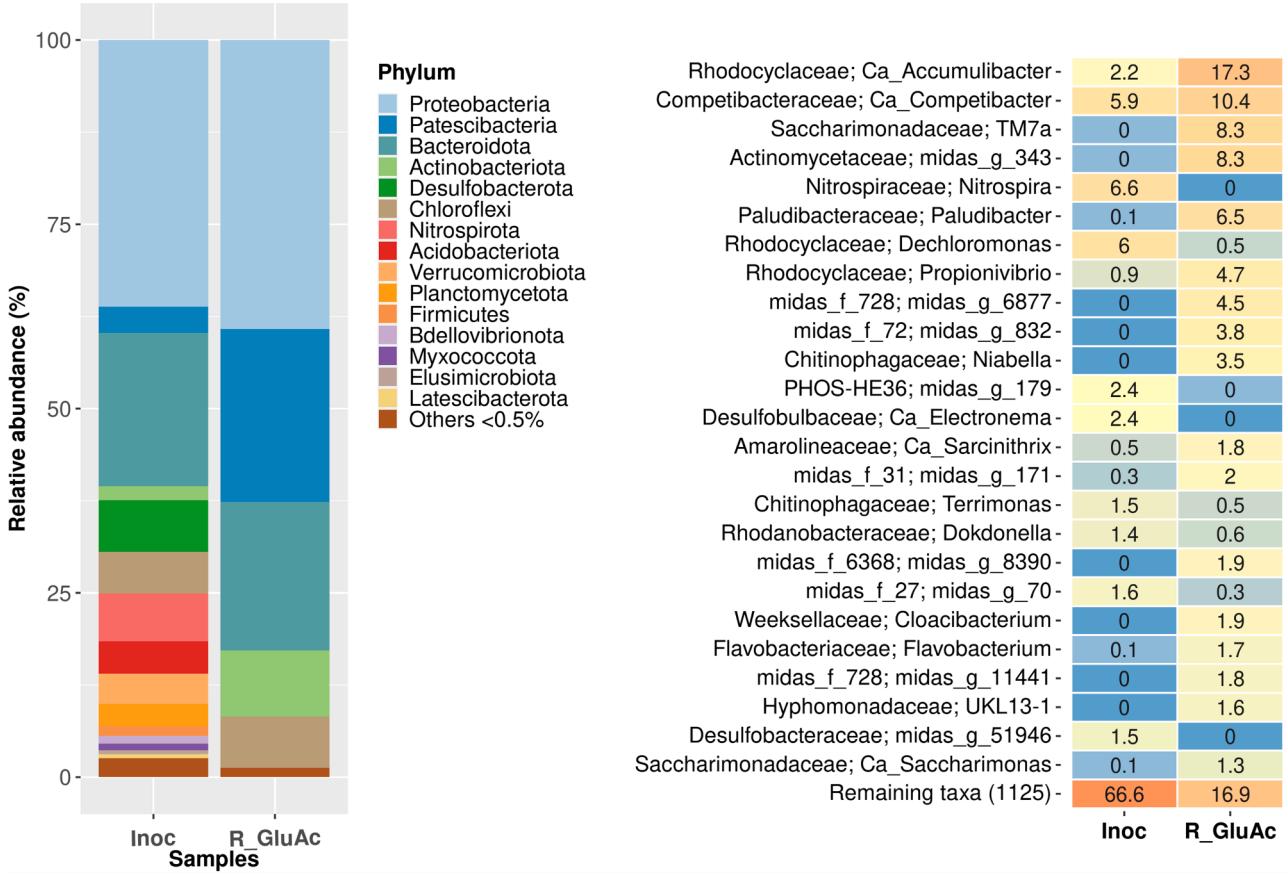

Fig. 5. Barplot of the relative abundance of the different phyla (left) and heatmap showing the most abundant genera (right) detected by 16S rRNA gene amplicon sequencing of the reactor after pseudo-steady-state conditions were reached (R_GluAc) and compared to the utilized inoculum (Inoc).

Table 3
Presence (in gray) or absence (in white) in the enriched culture of the expressed proteins involved in the glycolysis (Emden-Meyerhof-Parnas, EMP pathway), glycogen synthesis, and PHA synthesis in the four most abundant genera according to the performed metaproteome analysis.

Pathway	EC	Description	*Ca.* Accumulibacter	*Ca.* Contendobacter odensis	*Ca.* Competibacter denitrificans	*Ca.* Propionivibrio aalborgensis
Glycolysis (EMP pathway)	2.7.1.2	*glk,* glucokinase/hexokinase				
	5.3.1.9	*GPI,* glucose-6-phosphate isomerase				
	2.7.1.11	*pfkA,* 6-phosphofructokinase 1				
	4.1.2.13	*FBA,* fructose-bisphosphate aldolase class II				
	5.3.1.1	*TPI,* triosephosphate isomerase (TIM)				
	1.2.1.12	*gapA*, glyceraldehyde 3-phosphate dehydrogenase				
	2.7.2.3	*PGK*, phosphoglycerate kinase				
	5.4.2.12	*gpmI*, 2,3-bisphosphoglycerate-independent phosphoglycerate mutase				
	4.2.1.11	*ENO,* enolase				
	2.7.1.40	*PK*, pyruvate kinase				
Glycogen synthesis	5.4.2.2	*pgm,* phosphoglucomutase				
	2.7.7.27	*glgC,* glucose-1-phosphate adenylyltransferase				
	2.4.1.21	*glgA*, glycogen synthase				
	2.4.1.18	*glgB*, 1,4-alpha-glucan branching enzyme				
PHA synthesis	2.3.1.9	*phaA*, acetyl-CoA acetyltransferase				
	1.1.1.36	*phbB*, acetoacetyl-CoA reductase				
	2.3.1.304	*phaC*, polyhydroxyalkanoate synthase				
	4.2.1.119	*phaJ*, enoyl-CoA hydratase				
	5.4.99.2	*MUT*, methylmalonyl-CoA mutase				
	6.4.1.3	*pccA*, propionyl-CoA carboxylase alpha chain				
	2.1.3.15	*pccB*, propionyl-CoA carboxylase beta chain				

Table 4
Summary of the annotated MAGs of interest, including their taxonomic annotation and genome size, completeness, contamination, GC content, and N50.

Taxonomic annotation	Genome size (bp)	Completeness (%)	Contamination (%)	% GC	N50 (bp)
Rhodocyclaceae; Ca. Accumulibacter	2482,799	64.5	3.0	0.62	11,426
Rhodocyclaceae; Ca. Propionivibrio	4281,541	97.5	3.7	0.60	136,942
Competibacteraceae; Competibacter	3077,123	83.0	2.8	0.61	11,322
Competibacteraceae; Competibacter sp002433805	3910,889	96.0	2.8	0.61	122,140
Competibacteraceae; Ca, Contendobacter odensis	3450,364	92.1	1.5	0.59	18,904
Saccharimonadaceae	837,292	66.0	0	0.45	39,212
Saccharimonadaceae; TM7x	614,644	55.5	2.3	0.50	18,803
Saccharimonadaceae; Saccharimonas	649,565	62.6	3.4	0.48	5153
Saccharimonadaceae	851,307	60.4	0	0.45	74,332
Saccharimonadaceae; Saccharimonas sp0024221785	984,757	57.9	4.1	0.51	9906
Saccharimonadaceae	661,053	72.1	1.1	0.51	36,153

(Kuba et al., 1997a, 1997b; López-Vázquez et al., 2008). The P/C ratio of the cycle test (using glucose and acetate) was frequently higher than the reported values for lab-scale SBRs fed solely with acetate or comparable to (Schuler and Jenkins, 2003; Smolders et al., 1995).

Furthermore, the maximum P uptake rate was reported for the parent reactor and was higher than the reported values, except for the study of López-Vázquez et al. (2008) on full-scale WWTPs (30 to 88%). Likewise, the batch tests' P uptake rates were higher than most reported values. Combining the anaerobic and aerobic parameters, it was possible to assess that glucose and acetate's co-metabolism yielded the most favorable biological phosphorus removal results.

Regarding the operational conditions, the pH decreased during the anaerobic phases, consistent with the fermentation of glucose (Wang et al., 2001). The observed yield for the cycle test was 0.28 mg VSS/mg COD, and the phosphate content of the biomass, in this case, was 0.30 mg P/mg VSS. These results, in turn, signify a COD:P ratio of 100:9.3 (Table 7). Thus, the outcome is comparable to the COD:P ratio of *Ca.* Accumulibacter that was calculated using the growth yield of Wentzel et al. (1988) and the phosphate fraction of (Smolders et al., 1994a). Therefore, it also denotes the PAO-like behavior of the enriched community.

Table 5
Frequency of genes belonging to the glucose utilization pathways in the 11 annotated MAGs of interest.

Pathway	K number	*Ca.* Accumulibacter	*Ca.* Propionivibrio	*Ca.* Competibacter	*Ca.* Competibacter sp002433805	*Ca.* Contendobacter odensis	*Saccharimonadaceae*	*TM7x*	*Saccharimonas*	*Saccharimonadaceae*	*Saccharimonas* sp002421785	*Saccharimonadaceae*	EC	Genes
Glycolysis (EMP pathway)	K00845	1	1	0	0	0	0	0	0	0	0	0	2.7.1.2	*glk*
	K01810	1	1	1	1	1	0	0	0	0	0	0	5.3.1.9	*GPI, pgi*
	K00850	1	0	1	1	1	0	0	0	0	0	0	2.7.1.11	*pfkA, PFK*
	K01624	2	2	1	1	1	1	1	1	1	1	1	4.1.2.13	*FBA, fbaA*
	K01803	0	2	1	1	1	1	1	0	1	1	1	5.3.1.1	*TPI, tpiA*
	K00134	1	1	1	1	1	1	2	1	0	1	1	1.2.1.12	*gapA*
	K00927	0	1	1	1	1	1	1	0	1	1	1	2.7.2.3	*PGK*
	K15633	1	1	0	0	0	0	0	0	0	0	0	5.4.2.12	*gpmI*
	K01689	1	2	0	1	1	1	1	1	1	2	1	4.2.1.11	*ENO, eno*
	K00873	2	1	1	1	0	1	1	1	1	1	1	2.7.1.40	*PK, pyk*
	K01006	1	1	2	2	0	0	0	0	0	0	0	2.7.9.1	*PPDK*
Glycogen synthesis	K01835	1	1	1	1	1	0	0	0	0	0	0	5.4.2.2	*pgm*
	K00975	2	1	2	2	2	0	0	0	0	0	0	2.7.7.27	*glgC*
	K00703	1	1	1	1	1	0	0	0	0	0	0	2.4.1.21	*glgA*
	K00963	1	1	1	1	1	1	0	0	1	0	1	2.7.7.9	*UGP2, galU*
	K00700	3	2	3	6	3	2	0	0	1	1	2	2.4.1.18	*glgb*
Pyruvate oxidation	K00161	0	0	0	0	0	0	0	0	0	0	0	1.2.4.1	*PDHA, pdhA*
	K00162	0	0	0	0	0	0	0	0	0	0	0	1.2.4.1	*PDHB, pdhB*
	K00163	2	1	2	1	1	0	0	0	0	0	0	1.2.4.1	*aceE*
	K00627	1	1	1	1	0	0	0	0	0	0	0	2.3.1.12	*DLAT, aceF*
	K00382	1	3	2	3	0	0	0	0	0	0	0	1.8.1.4	*DLD, lpd*
	K13997	1	0	0	0	0	0	0	0	0	0	0	-	*PDHX*
	K00169	0	1	0	0	0	0	0	0	0	0	0	1.2.7.1	*porA*
	K00170	0	1	0	0	0	0	0	0	0	0	0	1.2.7.1	*porB*
	K00171	0	0	0	0	0	0	0	0	0	0	0	1.2.7.1	*porD*
	K00172	0	1	0	0	0	0	0	0	0	0	0	1.2.7.1	*porC, porG*
	K00189	0	0	0	0	0	0	0	0	0	0	0	1.2.7.1	*vorG, porG*
PHA synthesis	K00626	2	0	2	2	2	0	0	0	0	0	0	2.3.1.9	*atoB (phaA)*
	K00023	1	0	1	1	1	0	0	0	0	0	0	1.1.1.36	*phbB*
	K03821	1	0	3	2	5	0	0	0	0	0	0	2.3.1.304	*phaC, phbC*
	K19659	1	0	0	0	0	0	0	0	0	0	0	4.2.1.119	*phaJ*
	K01847	1	2	1	1	1	0	0	0	0	0	0	5.4.99.2	*MUT*
	K01965	1	1	2	1	0	0	0	0	0	0	0	6.4.1.3	*PCCA, pccA*
	K01966	1	3	1	1	1	0	0	0	0	0	0	2.1.3.15	*PCCB, pccB*

4.2. The role of ca. accumulibacter on glucose-fed systems

Several other studies that contradict the deteriorating effect of glucose in the EBPR process have been published, whether used as a supplement or, although less frequently, as a dominant substrate.

For instance, Wang et al. (2001) claimed a good EBPR performance using glucose as the primary substrate. Nevertheless, analyzing their results, the overall phosphate removed per 100 mg of COD consumed in the system was 100:3 after operational modifications (100:1.6 without the changes), which is not close to the COD:P ratio of 100:8 expected for a PAO culture, and closer to the 100:0.9 hypothesized to be used by OHOs to fulfill the growth requirements. Furthermore, as these studies did not report any community analysis, it is impossible to determine if the processes observed were performed by a single organism or via different microbial groups' synergy. Thus, in principle, the partial phosphate uptake observed in those systems could have been carried out via the partial fermentation of glucose into acetate by a fermentative organism, and the generated acetate could have been used by *Ca.* Accumulibacter for the removal of phosphate.

The study of Jeon and Park (2000) presented a good EBPR performance of an SBR supplied solely with glucose as the carbon source. They hypothesized that the overall process was carried out by two different

Table 6
Comparison of the stoichiometric and kinetic parameters of this study with reported values.

	$q^{MAX}_{COD,AN}$ (mg COD/g VSS h)	$q^{MAX}_{PO4,AN}$ (mg PO_4-P/g VSS h)	P/C ratio (mg PO_4-P /mg COD)	P/C ratio (mol P/ mol C)	$q^{MAX}_{PO4,\ Ox}$ (mg PO4-P/ g VSS h)	Reference
Cycle test (glucose and acetate)	50.0	19.9	0.44	0.45	18.6 7.8	This study
Batch test glucose	5.6	9.8	0.24	0.26	10.4 4.2	
Batch test acetate	40.1	19.1	0.50	0.52	12.5 6.4	
Full-scale WWTPs						
PAOs - modified UCT (full-scale system)	47.0	16.0	0.50		13.0	Kuba et al. (1997a, 1997b)
	19.0–22.0	11.1 −20.9	0.38 −0.45		9.0–19.2	López-Vázquez et al. (2008)
PAOs - Phoredox (full scale system)	11.0–21.0	9.6–20.9	0.33 −0.45		6.2–9.8	
PAOs – Sidestream PhoStrip (full-scale system)	9.0 23.0	10.4 6.0	0.40 0.31		9.8 2.2	Brdjanovic et al. (2000)

Table 7
Theoretical and experimental parameters for phosphorus calculations.

	OHOs	PAOs	This study
COD:P ratio (mg COD/mg P)	**100:0.9** Henze et al. (2008)	**100:8** Wentzel et al. (1988) Smolders et al. (1994a)	**100:9.3**
Growth yield (mg VSS/mg COD)	**0.45** Henze et al. (2008)	**0.21** Smolders et al. (1994a)	**0.28**
Phosphate fraction (f_P) (mg P/mg VSS)	**0.02** Henze et al. (2008)	**0.38** Wentzel et al. (1988)	**0.30**

microorganisms, namely PAOs and lactic acid-producing organisms (LPOs), and thus a new putative metabolic pathway was presented and inferred to occur when glucose is used. However, recent findings using lactate as the carbon source in the EBPR process that included microbial characterization have shown neither *Ca.* Accumulibacter nor *Tetrasphaera* can solely use lactate to remove phosphorus biologically (Rubio-Rincón et al., 2019).

Case in point, Santos et al. (1999) elucidated the metabolism of the PAO *Microlunatus phosphovorus* and discovered that this genus could ferment glucose into acetate while testing a pure culture, coinciding with the study of Nakamura et al. (1995). Moreover, it displayed high phosphorus release and uptake rates, although it was not capable of anaerobic growth (Santos et al., 1999). However, in our study, *M. phosphovorus* was not present in the 16S rRNA gene amplicon sequencing results or the proteomic analysis. Hence, the observed assimilation of glucose cannot be attributed to the presence in this species' culture. Moreover, as addressed below, the fermentation of glucose to acetate would generate an ATP molecule, thus lowering the need for hydrolyzing poly-P as the energy source.

Interestingly, the study presented here was dominated by *Ca.* Accumulibacter (67% according to the FISH analysis). Based on the 0.21 mg VSS/mg COD biomass growth yield reported by Smolders et al. (1994a) and our system's biomass concentration, it can be calculated that at least 80% of the available COD in the system had to be utilized by *Ca.* Accumulibacter, thus making it the dominant microorganism in the system. Since the acetate/glucose ratio was 1:1, this 80% COD consumption also signifies that the dominant member was either directly utilizing the glucose or relying on the presence of an ancillary secondary member fermenting the monosaccharide.

Nonetheless, the relative abundance considering the accounted ASVs (16S rRNA gene amplicon sequencing results) of all other putative PAOs, such as *Tetrasphaera, Dechloromonas, Microlunatus, Pseudomonas, Thiothrix, Halomonas*, and *Ca.* Obscuribacter either decreased compared to the inoculum, or the genus was absent from the reactor. Since the first can metabolize fermentable compounds, an increase in their abundance was expected (Kong et al., 2005; Kristiansen et al., 2013). The same can be said about GAOs, which can assimilate glucose. However, the utilized operational conditions (that proved to favor the growth of PAOs over GAOs in previous studies, i.e., pH of 7.0, OD of 20%, and an HRT of 16 h) seem to have successfully prevented the over-proliferation of GAOs in our system (Carvalheira et al., 2014; López-Vázquez et al., 2008). Hence, to the best of our knowledge, this is the first time a reactor enriched with *Ca.* Accumulibacter can putatively utilize glucose as the sole carbon source to biologically remove phosphate (5 mg/L of net P removal, COD: P (mg/mg) removal ratio of 100:6.3).

Lastly, the substantial discrepancy in relative abundance numbers observed between the two molecular methods has been discussed before by Rubio-Rincón et al. (2019) and Valverde-Pérez et al. (2016), who suggested that the studies should be supplemented with microbial activity measures. In this study, we carried out proteome and metagenome analyses to further elucidate the microbial composition and behavior.

4.3. Glucose utilization and storage

Concerning this study's phosphorus uptake, two rates were present for each cycle and batch test (Fig. 2, Table 1, and Fig. 3). The primary rate encompassed the first hour of aerobic conditions and was twice as big as the secondary rate. On the one hand, this fact coincides with the usual observations from systems enriched with *Ca.* Accumulibacter, where the phosphate uptake rate depends on the fraction of polyphosphate stored (Welles et al., 2017). However, as mentioned before, the 18.6 and 7.8 mg PO_4-P/g VSS h for the primary and secondary rates, respectively, indicate a noteworthy 58% difference, which has not been reported before.

According to the metabolism of *Ca.* Accumulibacter, the phosphate uptake capacity is not solely affected by the poly-P content (as described by Welles et al. (2017)) but is also affected by the utilization of the stored organic carbon (Henze et al., 2000). The recognized storage carbons or PAOs are mainly PHAs (PHB, PHV, PH_2MV, and PH_2MB) and glycogen. The PHA compound ultimately stored will depend on the carbon source utilized and the number of available electrons (Smolders et al., 1994a). For instance, if there are enough electrons for the uptake and conversion of acetate, then only PHB will be produced, and the TCA cycle is not needed (Fig. 6) (Guedes da Silva et al., 2020). Since this is usually not the case, the glyoxylate shunt is generally activated to produce reducing equivalents, and as a consequence, other PHAs are also produced (Guedes da Silva et al., 2020).

In line with this, different studies using propionate as the carbon

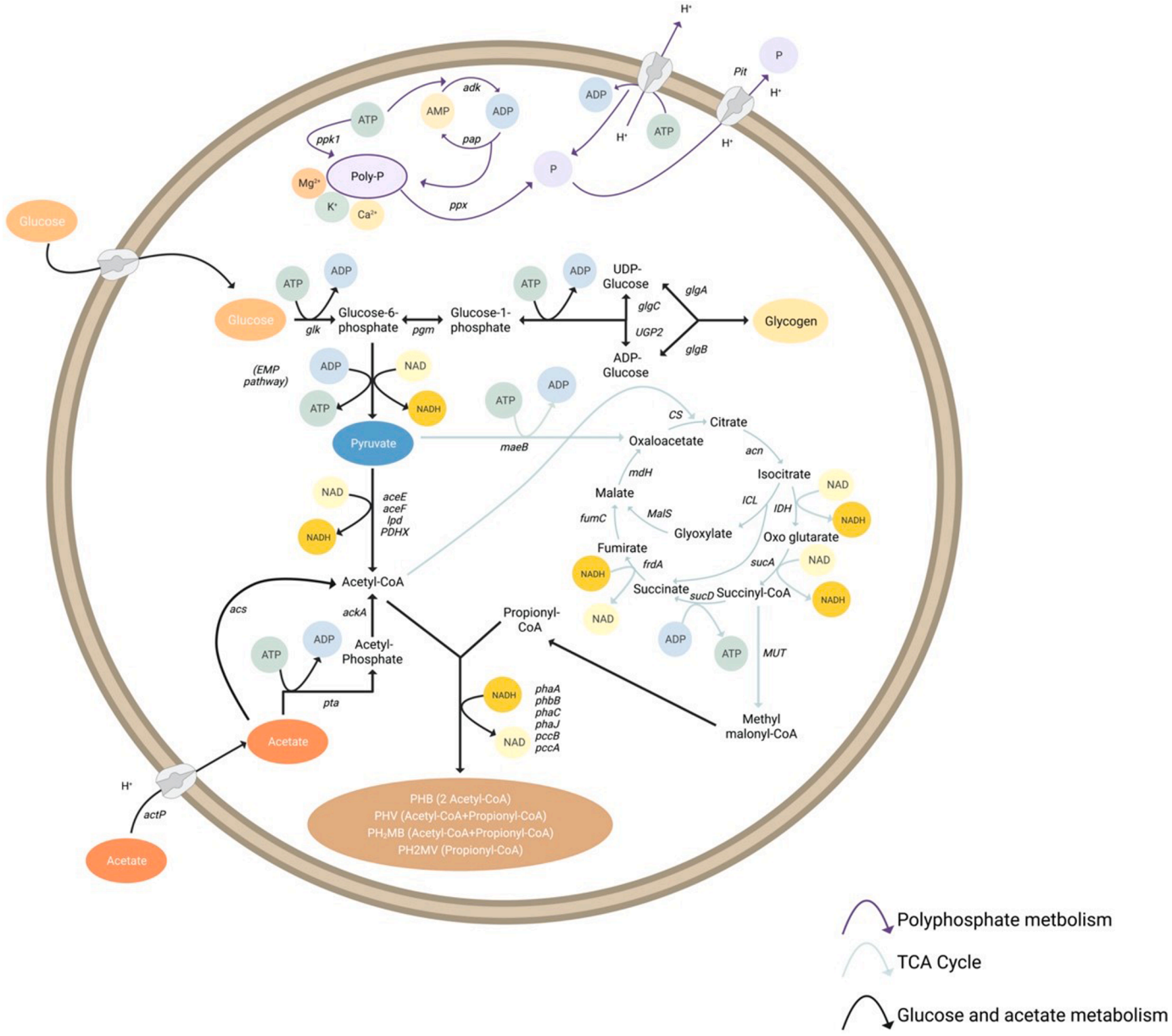

Fig. 6. Anaerobic metabolic model for *Ca.* Accumulibacter inferred from the enriched culture's phosphorus release and carbon consumption, together with the annotated MAG and metaproteomic analysis. The purple arrows symbolize the polyphosphate (poly-P) hydrolysis and phosphate (P) release, active when either acetate or glucose was provided. The blue arrows show the TCA cycle and the glyoxylate shunt, which could have been active during the production of PHAs if not enough reducing equivalents were present. The black arrows represent the acetate uptake and storage and the putative glucose uptake and direct storage. All of the stated genes were present in the annotated MAG of *Ca.* Accumulibacter.

Abbreviations: aceE, pyruvate dehydrogenase (EC: 1.2.4.1); aceF, pyruvate dehydrogenase (EC: 2.3.1.12); ackA, acetate kinase (EC: 2.7.2.1); acn, aconitate hydratase (EC: 4.2.1.3); acs, acetyl-CoA synthetase (EC: 6.2.1.1); actP, acetate symporter; adk, adenylate kinase (EC: 2.7.4.3); CS, citrate synthase (EC: 2.3.3.1); frdA, fumarate reductase (EC: 1.3.5.1); fumC, fumarate hydratase (EC: 4.2.1.2); glgA, glycogen synthase EC: 2.4.1.21); glgB, 1,4-alpha-glucan branching enzyme EC: 2.4.1.18); glgC, glucose-1-phosphate adenylyltransferase (EC: 2.7.7.27); glk, glucokinase (EC: 2.7.1.2); ICL, isocitrate lyase (EC: 4.1.3.1); IDH, isocitrate dehydrogenase (EC: 1.1.1.42); lpd, dihydrolipoamide dehydrogenase (EC: 1.8.1.4); maeB, malate dehydrogenase (EC: 1.1.1.40); MalS, malate synthase (EC: 2.3.3.9); mdH, malate dehydrogenase (EC: 1.1.1.37); MUT, methylmalonyl-CoA mutase (EC: 5.4.99.2); pap, polyP-AMP phosphotransferase (EC: 2.7.7.19); pccA, propionyl-CoA carboxylase alpha chain (EC: 6.4.1.3); pccB, propionyl-CoA carboxylase alpha chain (EC: 2.1.3.15); PDHX, dihydrolipoamide dehydrogenase-binding protein; pgm, phosphoglucomutase (EC: 5.4.2.2); phaA, acetyl-CoA acetyltransferase (EC: 2.3.1.9); phbB, acetyl-CoA reductase (EC: 1.1.1.36); phaC, polyhydroxyalkanoate synthase (EC: 2.3.1.304); phaJ, enoyl-CoA hydratase (EC: 4.2.1.119); Pit, low-affinity inorganic phosphate transporter; ppk1, polyphosphate kinase (EC: 2.7.4.1); ppx, exopolyphosphatase (EC: 3.6.1.11); pta, phosphate acetyltransferase (EC: 2.3.1.8); sucA, oxoglutarate dehydrogenase (EC: 1.2.4.2); sucD, succinyl-CoA synthethase (EC: 6.2.1.5); UGP2, UTP-glucose-1-phosphate uridylyltransferase (EC: 2.7.7.9) (created with BioRender.com).

source have generally reported slower phosphate uptake rates than studies fed with acetate (Oehmen et al., 2005; Rubio-Rincón et al., 2017). As acetate yields PHB and propionate, more reduced than the first, yields both PHB and PHV, the stored polymer could explain the aerobic phosphate uptake difference (Oehmen et al., 2005). Therefore, the change in aerobic uptake rates reported in this study could be explained by the presence of at least two organic storage polymers. The different oxidation rates of these polymers would, in turn, be reflected by a disparate phosphorus uptake rate. Nevertheless, contrary to propionate (which is more reduced than acetate), the oxidation state of

glucose is equal to acetate (Table 8). Thus, the formation of PHV from glucose via the known pyruvate-TCA cycle seems unlikely.

These results then lead to two hypothetical pathways. Either glucose is stored as glycogen or directly (or indirectly, fermented first to acetate by either *Ca*. Accumulibacter or the possible ancillary microorganisms) fermented to pyruvate and stored as PHA (Fig. 6). Analyzing these hypotheses by combining the results of the annotated MAG and the metaproteomic analysis, we found that all of the genes and enzymes involved in the EMP pathway of the glycolysis, glycogen synthesis, PHB, PHV, and PH_2MB synthesis, were either encoded or expressed by *Ca.* Accumulibacter (Tables 3 and 5), in accordance with previous reports (Kristiansen et al., 2013; Oyserman et al., 2016). Thus, from an enzymatic point of view, *Ca.* Accumulibacter expressed the necessary enzymes to store glucose as glycogen or PHA since the intracellular dynamics of both glycogen and PHA synthesis were induced, together with the generated phosphorus release and poly-P dynamics. Taking this into consideration, we propose the glucose utilization pathway by *Ca.* Accumulibacter as the most likely of the stated hypotheses (Fig. 6).

Moreover, it seems that the organism can perform both metabolic pathways (storage and fermentation of glucose). The turn-on/off function might depend on the anaerobically required and aerobically produced ATP. In this matter, metabolically speaking, storing glucose as PHA would generate ATP. On the other hand, storing glucose as glycogen would require ATP (Fig. 6). In principle, the ATP needed to store these compounds could be balanced by 50% of the glucose stored as glycogen and the remaining 50% stored as PHA. At the same time, the excess NADH produced via PHA storage could be utilized to form PHV and PH_2MV instead of PHB.

If that were the case, poly-P hydrolysis would be unnecessary as it only generates ATP during the process. Moreover, as a ratio of 0.26 mol P/mol C was observed in this study (batch test performed solely with glucose), it is not adequate postulation. Hence, considering that glucose is a C6 molecule and 1 mol of ATP is generated per mol of P hydrolyzed (Smolders et al., 1994b), *Ca.* Accumulibacter can generate 1.5 mol of ATP per mol of glucose via the poly-P hydrolysis and the mol P/mol C ratio observed in this study. Neglecting the ATP needed for other anaerobic processes (e.g., maintenance) infers that about 75% of the glucose could be stored as glycogen using the ATP provided via poly-P hydrolysis. The remaining 25% could be stored partially as glycogen and PHA by balancing its ATP utilization (glycogen generation) and formation (PHA storage).

As aforementioned, this should be related to the anaerobic ATP utilization and aerobic ATP formation. The ATP generation from an organic compound is related to its COD content and the carbon's oxidation state (Smolders et al., 1994b). Concerning this matter (as presented in Table 8), glycogen is more reduced than PHA. While, in principle, the COD is anaerobically conserved by the PAOs, the energy that could be generated from the oxidation of 1 mol of glycogen with respect to 1 mol of PHA would be higher. This difference, even if unlikely, could well explain why the observed growth yield of *Ca*. Accumulibacter in this study is higher than those reported in previous studies (Table 7). Finally, ATP's conservation would not be the only decisive factor in the storage polymer. Another potential factor would be the storage capacity of the organism. For instance, glycogen is stored within the cytoplasm, while PHA is stored as a long carbon chain. Hence, the storage of the first would occupy more space (as compared to PHA) within the available space of the organism and could play a significant role in further deciding how glucose could be stored, and as such, in influencing if the organism performs the hydrolysis of poly-P or not. Unfortunately, this study cannot unequally determine how much glucose has been stored as glycogen and how much as PHA. Hence, it is recommended that any follow-up studies should use C-labeled carbons.

5. Conclusions

A noteworthy EBPR performance in terms of phosphorous removal and overall kinetic and stoichiometric parameters was achieved in a lab-scale SRT fed with glucose and acetate (1:1 ratio). The dominant member was the microorganism *Ca.* Accumulibacter responsible for consuming approximately 80% of the fed carbon sources. The glucose was hypothesized to be directly stored by this organism predominantly as glycogen and partially as PHA, utilizing the ATP provided via the hydrolysis of poly-P and balancing its ATP utilization (glycogen generation) and formation (PHA storage). Other possible explanations are also discussed. To the best of our knowledge, this is the first report of a reactor enriched with *Ca.* Accumulibacter (relative FISH bio-abundance of 67 $\pm$ 5%) performing biological phosphorus removal putatively utilizing glucose as the sole carbon source (5 mg/L of net P removal, batch tests, COD:P (mg/mg) removal ratio of 100:6.3).

Table 8
The oxidation state of discussed compounds.

Compound	Chemical formula	Oxidation state
Glucose	$C_6H_{12}O_6$	0
Acetate	$C_2H_3O_2^-$	0
Glycogen	$(C_6H1_0O_5)n$	0
Pyruvate	$C_3H_4O_3$	- 2/3
PH3B	$(C_4H_6O_2)n$	1/2
PHV	$(C_5H_7O_2)n$	3/5

Declaration of Competing Interest

The authors declare that they have no known competing financial interests or personal relationships that could have appeared to influence the work reported in this paper.

Data availability

All data have been deposited in the Eawag Research Data Institutional Repository (https://opendata.eawag.ch/) and are publicly available.

Acknowledgments

This work was supported by the National Agency for Research and Innovation (ANII, Uruguay).

References

Albertsen, M., McIlroy, S.J., Stokholm-Bjerregaard, M., Karst, S.M., Nielsen, P.H., 2016. *Candidatus* Propionivibrio aalborgensis": a novel glycogen accumulating organism abundant in full-scale enhanced biological phosphorus removal plants. Front. Microbiol. 7 https://doi.org/10.3389/fmicb.2016.01033.

APHA, AWWA, WEF, 2005. Standard Methods For the Examination of Water and Wastewater. APHA-AWWA-WEF, Washington, D.C.

Barnard, J., 1975. Biological nutrient removal without addition of chemicals. Water Res. 9, 485–490. https://doi.org/10.1016/0043-1354(75)90072-X.

Barnard, J.L., Dunlap, P., Steichen, M., 2017. Rethinking the mechanisms of biological phosphorus removal. Water Environ. Res. 89, 2043–2054. https://doi.org/10.2175/106143017x15051465919010.

Begum, S.A., Batista, J.R., 2012. Microbial selection on enhanced biological phosphorus removal systems fed exclusively with glucose. World J. Microbiol. Biotechnol. 28, 2181–2193. https://doi.org/10.1007/s11274-012-1024-3.

Bolger, A.M., Lohse, M., Usadel, B., 2014. Trimmomatic: a flexible trimmer for Illumina sequence data. Methods 3, 2114–2120. https://doi.org/10.1093/bioinformatics/btu170.

Brdjanovic, D., van Loosdrecht, M.C.M., Versteeg, P., Hooijmans, C.M., Alaerts, G.J., Heijnen, J.J., 2000. Modeling COD, N and P removal in a full-scale WWTP Haarlem Waarderpolder. Water Res. 34 (3), 846–858. https://doi.org/10.1016/S0043-1354(99)00219-5.

Carvalheira, M., Oehmen, A., Carvalho, G., Eusébio, M., Reis, M.A.M., 2014. The impact of aeration on the competition between polyphosphate accumulating organisms and glycogen accumulating organisms. Water Res. 66, 296–307. https://doi.org/10.1016/j.watres.2014.08.033.

Cech, J.S., Hartman, P., 1993. Competition between polyphosphate and polysaccharide accumulating bacteria in enhanced biological phosphate removal systems. Water Res. 27, 1219–1225.

Cech, J.S., Hartman, P., 1990. Glucose induced break down of enhanced biological phosphate removal. Environ. Technol. 11, 651–656. https://doi.org/10.1080/09593339009384907.

Coats, E.R., Eyre, K., Bryant, C., Woodland, T., Brinkman, C.K., 2018. Assessing the effects of RAS fermentation on EBPR performance and associated microbial ecology. Water Environ. Res. 90, 659–671. https://doi.org/10.2175/106143017X15131012153130.

Comeau, Y., Hall, K.J., Hancock, R.E.W., Oldham, W.K., 1986. Biochemical model for enhanced biological phosphorus removal. Water Res. 20, 1511–1521. https://doi.org/10.1016/0043-1354(86)90115-6.

Crocetti, G.R., Banfield, F., JF, Keller, J., Bond, P.L., Blackall, L.L., 2002. Glycogen-accumulating organisms in laboratory-scale and full-scale wastewater treatment processes. Microbiology 148, 3353–3364. https://doi.org/10.1099/00221287-148-11-3353.

Crocetti, G.R., Hugenholtz, P., Bond, P.L., Schuler, A., Keller, J., Jenkins, D., Blackall, L. L., 2000. Identification of polyphosphate-accumulating organisms and design of 16S rRNA-directed probes for their detection and quantitation. Appl. Environ. Microbiol. 66, 1175–1182. https://doi.org/10.1128/AEM.66.3.1175-1182.2000.

Dueholm, M.S., Nierychlo, M., Andersen, K.S., Rudkjøbing, V., Knutsson, S., Consortium, the M.G., Albertsen, M., Nielsen, P.H., 2021. MiDAS 4: a global catalogue of full-length 16S rRNA gene sequences and taxonomy for studies of bacterial communities in wastewater treatment plants. bioRxiv 2021.07.06.451231. https://doi.org/10.1101/2021.07.06.451231.

Gebremariam, S.Y., Beutel, M.W., Christian, D., Hess, T.F., 2012. Effects of glucose on the performance of enhanced biological phosphorus removal activated sludge enriched with acetate. Bioresour. Technol. 121, 19–24. https://doi.org/10.1016/j.biortech.2012.06.086.

Guedes da Silva, L., Gamez, O., Gomes, C., Akkermans, K., Welles, L., Abbas, B., van Loosdrecht, M.M.C., Aljosscha Wahl, S., 2020. Revealing the metabolic flexibility of "Candidatus Accumulibacter phosphatis" through redox cofactor analysis and metabolic network modeling. Appl. Environ. Microbiol. 86.

Henze, M., Gujer, W., Mino, T., van Loosdrecht, M., 2000. Activated Sludge Models ASM1, ASM2, ASM2D, ASM3, Water Intelligence Online. https://doi.org/10.2166/9781780402369.

Herlemann, D.P.R., Labrenz, M., Jürgens, K., Bertilsson, S., Waniek, J.J., Andersson, A.F., 2011. Transitions in bacterial communities along the 2000 km salinity gradient of the Baltic Sea. ISME J. 5, 1571–1579. https://doi.org/10.1038/ismej.2011.41.

Jeon, C.O., Park, J.M., 2000. Enhanced biological phosphorus removal in a sequencing batch reactor supplied with glucose as a sole carbon source. Water Res. 34, 2160–2170. https://doi.org/10.1016/S0043-1354(99)00383-8.

Kanehisa, M., Goto, S., 2000. KEGG: kyoto encyclopedia of genes and genomes. Nucleic Acids Res. 28, 27–30. https://doi.org/10.1093/nar/28.1.27.

Kleikamp, H.B.C., Pronk, M., Tugui, C., da Silva, L.G., Abbas, B., Lin, Y.M., van Loosdrecht, M.C.M., Pabst, M., 2020. Quantitative profiling of microbial communities by *de novo* metaproteomics. bioRxiv 2020.08.16.252924. https://doi.org/10.1101/2020.08.16.252924.

Kong, Y., Nielsen, J.L., Nielsen, P.H., 2005. Identity and ecophysiology of uncultured actinobacterial polyphosphate-accumulating organisms in full-scale enhanced biological phosphorus removal plants. Appl. Environ. Microbiol. 71, 4076–4085. https://doi.org/10.1128/AEM.71.7.4076-4085.2005.

Kong, Y., Nielsen, J.L., Nielsen, P.H., 2004. Microautoradiographic study of *Rhodocyclus*-related polyphosphate-accumulating bacteria in full-scale enhanced biological phosphorus removal plants. Appl. Environ. Microbiol. 70 https://doi.org/10.1128/AEM.70.9.5383-5390.2004, 5383 LP –5390.

Kristiansen, R., Nguyen, H.T.T., Saunders, A.M., Nielsen, J.L., Wimmer, R., Le, V.Q., McIlroy, S.J., Petrovski, S., Seviour, R.J., Calteau, A., Nielsen, K.L., Nielsen, P.H., 2013. A metabolic model for members of the genus *Tetrasphaera* involved in enhanced biological phosphorus removal. ISME J. 7, 543–554. https://doi.org/10.1038/ismej.2012.136.

Kuba, T., Van Loosdrecht, M.C.M., Brandse, F.A., Heijnen, J.J., 1997a. Occurrence of denitrifying phosphorus removing bacteria in modified UCT-type wastewater treatment plants. Water Res. 31, 777–786. https://doi.org/10.1016/S0043-1354(96)00370-3.

Kuba, T., van Loosdrecht, M.C.M., Murnleitner, E., Heijnen, J.J., 1997b. Kinetics and stoichiometry in the biological phosphorus removal process with short cycle times. Water Res. 31, 918–928. https://doi.org/10.1016/S0043-1354(96)00371-5.

Li, D., Luo, R., Liu, C.-.M., Leung, C.-.M., Ting, H.-.F., Sadakane, K., Yamashita, H., Lam, T.-.W., 2016. MEGAHIT v1.0: a fast and scalable metagenome assembler driven by advanced methodologies and community practices. Methods 102, 3–11. https://doi.org/10.1016/j.ymeth.2016.02.020.

Liu, W.-.T., Nielsen, A.T., Wu, J.-.H., Tsai, C.-.S., Matsuo, Y., Molin, S., 2001. *In situ* identification of polyphosphate- and polyhydroxyalkanoate-accumulating traits for microbial populations in a biological phosphorus removal process. Environ. Microbiol. 3, 110–122. https://doi.org/10.1046/j.1462-2920.2001.00164.x.

López-Vázquez, C.M., Hooijmans, C.M., Brdjanovic, D., Gijzen, H.J., van Loosdrecht, M. C.M., 2008. Factors affecting the microbial populations at full-scale enhanced biological phosphorus removal (EBPR) wastewater treatment plants in The Netherlands. Water Res. 42, 2349–2360. https://doi.org/10.1016/j.watres.2008.01.001.

Marques, R., Santos, J., Nguyen, H., Carvalho, G., Noronha, J.P., Nielsen, P.H., Reis, M.A. M., Oehmen, A., 2017. Metabolism and ecological niche of *Tetrasphaera* and *Ca.* Accumulibacter in enhanced biological phosphorus removal. Water Res. 122, 159–171. https://doi.org/10.1016/j.watres.2017.04.072.

McMurdie, P.J., Holmes, S., 2013. phyloseq: an r package for reproducible interactive analysis and graphics of microbiome census data. PLoS ONE 8, e61217.

Mino, T., Satoh, H., Matsuo, T., 1994. Metabolisms of different bacterial populations in enhanced biological phosphate removal processes. Water Sci. Technol. 29, 67–70. https://doi.org/10.2166/wst.1994.0309.

Mino, T., Van Loosdrecht, M.C.M., Heijnen, J.J., 1998. Microbiology and biochemistry of the enhanced biological phosphate removal process. Water Res. 32, 3193–3207. https://doi.org/10.1016/S0043-1354(98)00129-8.

Nakamura, K., Hiraishi, A., Yoshimi, Y., Kawaharasaki, M., Masuda, K., Kamagata, Y., 1995. *Microlunatus phosphovorus* gen . nov ., sp . nov ., a new Gram-positive polyphosphate-accumulating bacterium isolated from activated sludge. Int. J. Syst. Bacteriol. 45, 17–22.

Nguyen, H.T.T., Le, V.Q., Hansen, A.A., Nielsen, J.L., Nielsen, P.H., 2011. High diversity and abundance of putative polyphosphate-accumulating *Tetrasphaera*-related bacteria in activated sludge systems. FEMS Microbiol. Ecol. 76, 256–267. https://doi.org/10.1111/j.1574-6941.2011.01049.x.

Nielsen, P., 2009. FISH handbook for biological wastewater treatment. Water Intell. Online 8. https://doi.org/10.2166/9781780401775.

Oehmen, A., Lemos, P.C., Carvalho, G., Yuan, Z., Keller, J., Blackall, L.L., Reis, M.A.M., 2007. Advances in enhanced biological phosphorus removal: from micro to macro scale. Water Res. 41, 2271–2300. https://doi.org/10.1016/j.watres.2007.02.030.

Oehmen, A., Yuan, Z., Blackall, L.L., Keller, J., 2005. Comparison of acetate and propionate uptake by polyphosphate accumulating organisms and glycogen accumulating organisms. Biotechnol. Bioeng. 91, 162–168. https://doi.org/10.1002/bit.20500.

Oyserman, B.O., Noguera, D.R., del Rio, T.G., Tringe, S.G., McMahon, K.D., 2016. Metatranscriptomic insights on gene expression and regulatory controls in *Candidatus* Accumulibacter phosphatis. ISME J 10, 810–822. https://doi.org/10.1038/ismej.2015.155.

Parks, D.H., Chuvochina, M., Chaumeil, P.-.A., Rinke, C., Mussig, A.J., Hugenholtz, P., 2020. A complete domain-to-species taxonomy for Bacteria and Archaea. Nat. Biotechnol. 38, 1079–1086. https://doi.org/10.1038/s41587-020-0501-8.

Randall, A.A., Benefield, L.D., Hill, W.E., Nicol, J.-.P., Boman, G.K., Jingo, S.-.R., 1997. The effect of volatile fatty acids on enhanced biological phosphorus removal and population structure in anaerobic/aerobic sequencing batch reactors. Water Sci. Technol. 35, 153–160. https://doi.org/10.1016/S0273-1223(96)00891-8.

Rubio-Rincón, F.J., López-Vázquez, C.M., Welles, L., van Loosdrecht, M.C.M., Brdjanovic, D., 2017. Cooperation between Candidatus Competibacter and Candidatus Accumulibacter clade I, in denitrification and phosphate removal processes. Water Res. 120, 156–164. https://doi.org/10.1016/j.watres.2017.05.001.

Rubio-Rincón, F.J., Welles, L., Lopez-Vazquez, C.M., Abbas, B., Van Loosdrecht, M.C.M., Brdjanovic, D., 2019. Effect of lactate on the microbial community and process performance of an EBPR system. Front. Microbiol. 10, 1–11. https://doi.org/10.3389/fmicb.2019.00125.

Santos, M.M., Lemos, P.C., Reis, M.A.M., Santos, H., 1999. Glucose metabolism and kinetics of phosphorus removal by the fermentative bacterium *Microlunatus phosphovorus*. Appl. Environ. Microbiol. 65 https://doi.org/10.1128/AEM.65.9.3920-3928.1999, 3920 LP –3928.

Schuler, A.J., Jenkins, D., 2003. Enhanced biological phosphorus removal from wastewater by biomass with different phosphorus contents, Part I: experimental results and comparison with metabolic models. Water Environ. Res. 75, 485–498.

Smolders, G.J.F., van der Meij, J., van Loosdrecht, M.C.M., Heijnen, J.J., 1994a. Model of the anaerobic metabolism of the biological phosphorus removal process: stoichiometry and pH influence. Biotechnol. Bioeng. 43, 461–470. https://doi.org/10.1002/bit.260430605.

Smolders, G.J.F., van der Meij, J., van Loosdrecht, M.C.M., Heijnen, J.J., 1994b. Stoichiometric model of the aerobic metabolism of the biological phosphorus removal process. Biotechnol. Bioeng. 44, 837–848. https://doi.org/10.1002/bit.260440709.

Smolders, G.J.F., van Loosdrecht, M.C.M., Heijnen, J.J., 1995. A metabolic model for the biological phosphorus removal process. Water Sci. Technol. 31, 79–93. https://doi.org/10.1016/0273-1223(95)00182-M.

Smolders, G.J.F., Van Loosdrecht, M.C.M., Heijnen, J.J., 1996. Steady-state analysis to evaluate the phosphate removal capacity and acetate requirement of biological phosphorus removing mainstream and sidestream process configurations. Water Res. 30, 2748–2760. https://doi.org/10.1016/S0043-1354(96)00127-3.

Uritskiy, G.V., DiRuggiero, J., Taylor, J., 2018. MetaWRAP—A flexible pipeline for genome-resolved metagenomic data analysis. Microbiome 6, 158. https://doi.org/10.1186/s40168-018-0541-1.

Valverde-Pérez, B., Wágner, D.S., Lóránt, B., Gülay, A., Smets, B.F., Plósz, B.G., 2016. Short-sludge age EBPR process – Microbial and biochemical process characterisation during reactor start-up and operation. Water Res. 104, 320–329. https://doi.org/10.1016/j.watres.2016.08.026.

Wang, N., Peng, J., Hill, G., 2002. Biochemical model of glucose induced enhanced biological phosphorus removal under anaerobic condition. Water Res. 36, 49–58. https://doi.org/10.1016/S0043-1354(01)00236-6.

Wang, N., Peng, J., Hill, G., 2001. The role of glucose in developing enhanced biological phosphorus removal. Environ. Eng. Pol. 3, 45–54. https://doi.org/10.2175/193864700785156307.

Wang, Y., Jiang, F., Zhang, Z., Xing, M., Lu, Z., Wu, M., Yang, J., Peng, Y., 2010. The long-term effect of carbon source on the competition between polyphosphorus accumulating organisms and glycogen accumulating organism in a continuous plug-flow anaerobic/aerobic (A/O) process. Bioresour. Technol. 101, 98–104. https://doi.org/10.1016/j.biortech.2009.07.085.

Welles, L., Abbas, B., Sorokin, D.Y., Lopez-Vazquez, C.M., Hooijmans, C.M., van Loosdrecht, M.C.M., Brdjanovic, D., 2017. Metabolic response of "*Candidatus*

Accumulibacter phosphatis" clade II C to changes in influent P/C ratio. Front Microbiol.
Wentzel, M.C., Ekama, G.A., Dold, P.L., Loewenthal, R.E., Marais, G., 1988. Biological Excess Phosphorus Removal, 148. University of Cape Town.
Wentzel, M.C., Lotter, L.H., Loewenthal, R.E., Marais, G., 1986. Metabolic behaviour of *Acinetobacter* spp. in enhanced biological phosphorus removal - a biochemical model. Water SA 12, 209–224.